Pediatric Coronal Suture Fiber Alignment and the Effect of Interdigitation on Coronal Suture Mechanical Properties

Kelly Nicole Adamski, Andre Matthew Loyd, Albert Samost, Barry Myers, Roger Nightingale, Kathleen Smith & Cameron R. 'Dale' Bass

Springer

Springer

BMES
BIOMEDICAL ENGINEERING SOCIETY™
www.bmes.org

Pediatric Coronal Suture Fiber Alignment and the Effect of Interdigitation on Coronal Suture Mechanical Properties

Kelly Nicole Adamski,[1,2] Andre Matthew Loyd,[1] Albert Samost,[1] Barry Myers,[1] Roger Nightingale,[1] Kathleen Smith,[2] and Cameron R. 'Dale' Bass[1]

[1]Department of Biomedical Engineering, Injury and Orthopaedic Biomechanics Laboratory, Duke University, Box 90281, Durham, NC 27708-0281, USA; and [2]Department of Biology, Duke University, Box 90338, Durham, NC 27708-0281, USA

Associate Editor Kent Leach oversaw the review of this article.

Abstract—The morphological and mechanical properties of the pediatric skull are important in understanding pediatric head injury biomechanics. Although previous studies have analyzed the morphology of cranial sutures, none has done so in pediatric specimens nor have previous studies related the morphology to mechanical properties of human sutures. This study quantified the geometry of pediatric cranial sutures and investigated its correlation with the suture mechanical properties. First, the suture fiber alignment was quantified using histological analysis for four ages—neonate, 9 months-old, 11 months-old, and 18 months-old. For the morphometric investigation of the suture interdigitation, suture samples from a 6-year-old were scanned using micro-CT and the level of interdigitation was measured using two techniques. The first technique, the sinuosity index, was calculated by dividing the suture path along the surface of the skull by the suture distance from beginning to end. The second technique, the surface area interdigitation index, was calculated by measuring the surface area of the bone interface outlining the suture and dividing it by the cross-sectional area of the bone. The mechanical properties were obtained using methods reported in Davis *et al.*[6]. The results of the histological analysis showed a significant increase in fiber alignment in older specimen; where random fiber alignment has an average angle deviation of 45°, neonatal suture fibers have an average deviation of 32.2° and the 18-month-old fibers had an average deviation of 16.2° ($p < 0.0001$). For the suture index measurements, only the sinuosity was positively correlated with the ultimate strain ($R^2 = 0.62$, Bonferroni corrected $p = 0.011$) but no other measurements showed a significant relationship, including the amount of interdigitation and elastic modulus. Our results demonstrate that there is a distinct developmental progression of the suture fiber alignment at a young age, but the differences in suture interdigitation can only predict the ultimate strain and no other mechanical properties.

Keywords—Sutures, Interdigitation, Fibers, Pediatric, Skull, Morphology, Fracture, Mechanical properties.

INTRODUCTION

The study of the biomechanics of childhood head injury is hindered by a limited understanding of the material properties of the pediatric skull, especially the mechanical and morphological properties of the pediatric suture. Previous studies have primarily focused on the morphology and patterns at the interface of the suture, with a few studies evaluating the mechanical properties of the sutures and their relationship with morphology.[3,11]

The morphological studies of human cranial sutures have recognized a qualitative change in the local suture structure throughout a lifetime. At birth, sutures of the cranial vault must permit some flexibility to accommodate a shift of the cranial bones during passage through the birth canal and remain as active growth and signaling centers into the early years of life.[24] The suture is soft, pliable and unable to support a bending moment during these ages. Calvarial sutures become more rigidly connected through fusion at 18 months and ossification after 22–26 years.[5] Ultimately, cranial sutures ossify, contributing to the strength of the skull and its ability to protect the brain.[9] The increase in strength is believed to be caused by type I collagen which spans across the length of the suture mesenchyme.[1,7,25] The current theory is that the stiffness of the suture increases with age due to the fibers becoming more aligned.[7,23] This has been observed and

Address correspondence to Andre Matthew Loyd, Department of Biomedical Engineering, Injury and Orthopaedic Biomechanics Laboratory, Duke University, Box 90281, Durham, NC 27708-0281, USA. Electronic mails: kelly.adamski@gmail.com, Andre.M.Loyd@gmail.com, alsamost@gmail.com, bsm@duke.edu, lrwn@duke.edu, kksmith@duke.edu, and dale.bass@duke.edu

reported in various studies but has been limited in human pediatric specimens and without quantification.[1,13,20,22]

Another morphometric characteristic of the sutures is the jagged suture path described as the interdigitation of the suture, which provides a distinct attribute to the geometry of the suture. Interdigitating becomes pertinent once the two encroaching bones fuse and the suture can support a bending moment. In 1990, Jaslow defined the interdigitation index as a way to quantify the physical interdigitation in goat cranial sutures, calculated by dividing the jagged suture path by the straight distance.[11] The work measured the interdigitation index along the skull surface, now referred to as the sinuosity, and found a positive correlation between interdigitation index, and bending strength and energy absorbed, or the total energy sustained by the suture before failure.[11] From this, they hypothesized that the suture serves as shock absorbers for the skull.[12] Rafferty and Herring modified the interdigitation index and measured it from ectocranial to endocranial surface from histological slides, looking at the cross-section of porcine sutures. Their work compared suture morphology to *in vivo* strain, observing a relationship between *in vivo* compressive strain and interdigitation.[22] Most recently, Markey and Marshall[17,18] used Micro-CT to assess the morphology of cranial sutures in the fish *Polypterus endlicherii*, which included the interdigitation index from the ecto- to endocranial skull surface and connected the morphology to the type of stresses (tension or compression) that the suture experiences, but did not connect the data to mechanical properties.[17–19] Still, there are differing theories about the role of interdigitation in suture development. Jaslow theorized that an increase in suture interdigitation could provide an increase in surface area at the suture interface and therefore an increase in possible anchor points for the collagen fibers of the suture mesenchyme, causing a higher tensile strength for the suture.[11] Herring hypothesized that an increase in interdigitation increases the bone-bone interactions as the suture is bent, which could provide additional resistance to deformation.[8] Markey *et al.* hypothesized that suture becomes more interdigitated when the joint mainly resist compression.[17] Nevertheless, no study has related the interdigitation to the mechanical properties of the human suture.

Only three studies have evaluated the mechanical properties of the human cranial sutures in infant and young pediatric specimens. Margulies and Thibault performed the first experiments to determine the mechanical properties of human pediatric sutures less than 6-month-old.[16] Coats and Margulies followed that study with specimens less than 1-year-old.[4] Their data were limited owing to a lack of specimen avail-

ability and small sample size, and they found no direct correlation between age and elastic modulus, though there was a significant interaction of strain rate and age on elastic modulus.[4] Most recently, Davis *et al.* tested the sutures of a 6-year-old.[6] They found that the suture was indeed weaker than the surrounding bone at that age and that the bone and suture failed at the same strain levels. Davis also found that there were no statistical difference in mechanical properties coronal and lambdoid sutures. However, neither study evaluated morphological and mechanical properties link. These studies were the first to provide biomedical data on sutures; to date, no study has examined the effect of morphological variation within the coronal suture of one individual or across individuals of different ages. Further, there are no studies quantifying local fiber variation in pediatric sutures.

A better understanding of the morphology of the pediatric skull can provide insight into how interdigitation and fiber alignment relate to mechanical properties. Hence, this study investigates two alternate components that contribute to the morphology of the sutures—suture fiber alignment and interdigitation of the bone fronts, measured through histology and micro-CT respectively. This study measures gross anatomic features to quantify the alignment of suture fibers and apply measurements of the interdigitation index to the sutures of the human skull. The sutural interdigitation measurements, including the sinuosity and the novel surface area interdigitation index, are compared to measured mechanical properties of the suture to identify any correlations. We hypothesize that (1) older specimens have a local mean fiber direction that is more aligned than younger specimens from birth to 18 months and (2) larger interdigitation indices correlate with an increase in the modulus of elasticity and energy absorbed.

MATERIALS AND METHODS

Two studies were conducted; one was a histological analysis of coronal sutures from two neonate, one 9-month-old, one 11-month-old, and one 18-month-old. This was followed by a study of the interdigitation of the suture from one 6-year-old specimen that was used in a previous suture study.[6]

Fiber Alignment: Histological Preparation

Pediatric cadaver heads were obtained in compliance with federal, state, local and institutional regulations. No instructional review board approval was needed for post mortem human subjects. The heads were frozen at −20° until they underwent non-

destructive head and neck tests unrelated to this research. Once testing was complete, suture samples were removed from the superior coronal suture (closest to the fontanelle) for histological and mechanical analysis. The samples from the 6-year-old for mechanical testing were taken along the entire length of the right and left coronal sutures. Then coronal suture samples were selected from each specimen for the histological study, submersed in 0.9% NaCl saline and stored in $-20°$ freezer until later use. Samples were thawed and fixed in 10% buffered formalin overnight, decalcified, and embedded on edge in paraffin. Suture samples were sliced along the sagittal plane 5–7 μm thick and removed in a step-wise fashion, with one step equaling 20 μm. Slides were stained with Masson's trichrome and hematoxylin and eosin, which have been used previously in studies of cranial tissue fiber composition.[15,21]

Fiber Alignment: Quantification

One representative slide from each suture sample was selected that was adequately stained to identify the bone and suture and had minimal tearing due to handling. Then the sections were viewed with light microscope (Nikon Eclipse TE2000-U, Melville, NY) and digital images were obtained using the attached camera and NIS-Element image-capturing software (Nikon Advantage, Melville, NY). Sections were viewed at 20$\times$ and photographs were taken in small frames and stitched together using camera software. Five 150 μm $\times$ 150 μm viewing frames were randomly selected from suture mesenchyme region. The viewing frame was rejected if more than 50% of the selected area contained bone, dura mater, or pericranium instead of suture mesenchyme.

The slopes of the fibers in each viewing frame were measured in reference to the horizontal edge of the image, where the 0° angle was a starting reference value. All slopes were converted to their angle measurement, and the resulting angles were renormalized relative to the median angle for analysis; therefore, for all the analyses, 0° approximates the direct fiber line between the frontal and parietal bone. To account for the structural sameness of $+90°$ and $-90°$ measurements, the absolute value of the angle deviations were calculated, therefore all measurements were between 0° and 90°. The mean of the angle measurements were calculated. Using this methodology, completely random fiber alignment would have a mean angle measurement of 45°.

Interdigitation: Micro-CT Imaging and Sinuosity

Twelve coronal suture samples from one 6-year-old specimen were removed and micro-CT scanned at 50 μm resolution prior to testing in four-point bend testing.[6] The sample were wrapped in saline-soaked gauze during the micro-CT scans. The micro-CT scans were converted into a three-dimensional mesh using Avizo 6.0 (Visualizations Sciences Group, Burlington, MA). The sinuosity index was calculated from the 3-D mesh by setting points along the ectocranial surface of the skull and converting those points to a 50-point spline curve (Fig. 1). Distances between consecutive points were calculated and summed to find the length of the suture path. Suture path was divided by the distance between the first and last point to calculate the sinuosity index.

Interdigitation: Image Conversion and Surface Area Index

The images in each CT slice were segmented into frontal bone and parietal bone complements of the suture and transformed into 3-D solid meshes using Avizo 6.0. These solids were exported into Hypermesh (Altair, Troy, MI) where the complementary bone faces of the suture were separated and interdigitation surfaces were selected. Only the surface components of each interacting bone face were selected for surface area calculations and the sides were not taken into account along with any surface components which were both part of the side and periosteum faces (Fig. 2). Then, the segmented solids were exported to LS-DYNA (Livermore Software Technology Corp., Livermore, CA) where the surface area of the interdigitation was calculated (Fig. 2). The surface area calculations of the two fronts were averaged together to get the interdigitation surface area. Since, the inner and outer table merge at the suture area, the cross-sectional area was found by multiplying the height by the width of the bone measured *via* Hypermesh (Fig. 2). The surface area interdigitation index was calculated by dividing the interdigitation surface area by the cross sectional surface area.

Mechanical Properties Data

Mechanical properties data for the suture segments used was obtained using the following methods.[6] Bending tests were performed using a Bose Electroforce 3200 linear actuator and a custom-built four point rig. The displacement was measured by the internal LVDT and the force measured by the Honeywell Model-31 222.5 N load cell. Each failure test was video recorded and the video was later used for the analysis. The suture was assumed to behave like a solid beam with an unchanging cross-section and stress estimated using the beam bending equation,
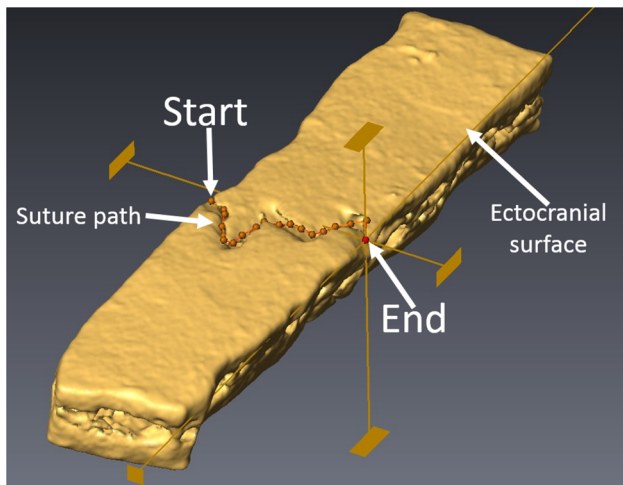
FIGURE 1. Measuring the sinuosity. The image is of a sample coronal suture illustrating how the sinuosity of the suture is measured. The measurement was done on the ectocranial surface by dividing the entire length of the suture path by the distance between the start and end points as shown. Micro-CT scans were loaded into Avizo 6.0 and converted to a 3-D mesh. Three-dimensional points were placed along the suture and converted to a spline to obtain the suture path.

$$\sigma = \frac{My}{I}$$

where M is the bending moment, y is the half thicknesses and I is the moment of inertia of the cross-section. Each suture sample was tested with the periosteal side of the suture in compression which allowed suture to become less curved during the bending tests. The tensile strain on the suture was calculated by tracking the radius of curvature using the angle of rotation of the end pieces and using the equation:

$$\varepsilon = \frac{2y\theta}{L}$$

where y is the half-thickness, L is the original suture sample length and θ is the angle of rotation. The modulus of elasticity, yield stress and yield strain were calculated by using a Ramberg–Osgood piecewise linear and power law curve fit with a 0.2% offset as the cutoff for linearity. For this analysis, we were interested in the overall response of the suture joint, not just the fibers of the suture joint. Hence, modulus of elasticity calculations should be considered the effective modulus of the suture structure. Additionally, ultimate stress and ultimate strain was calculated for each sample using the stress-strain curve. Ultimate stress represents the maximum force per unit area that the suture can withstand before failure while ultimate strain measures the maximum deformation the suture experiences before failure. Finally, energy absorbed is measured by calculating the area under the force-deflection curve.
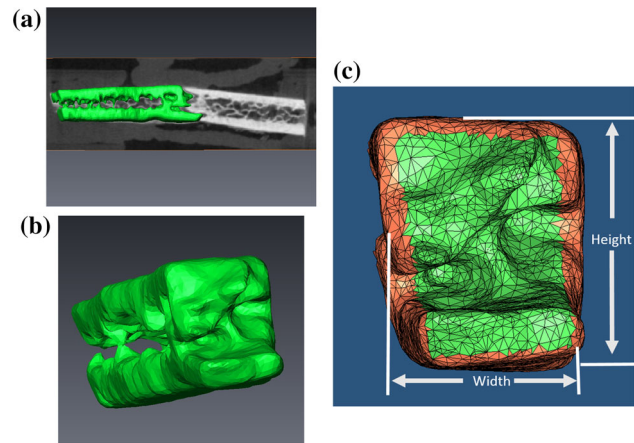

FIGURE 2. Images used to measure surface area interdigitation index. The surface area of the interdigitation is denoted by the green elements in figure c. The area surface area of interdigitation was divided the cross-sectional area of suture (width × height) to get the suture area interdigitation index. (a) Using Avizo 6.0 imaging software, a 3-D mesh (green) was created from micro-CT scans of bone-suture-bone strips (b) Two bones outlining suture were separated to observe suture interface (c) Using LS-DYNA, surface area was measured from both bone segments and excluded the top, bottom, and sides of the bone strip.

Statistical Analysis

By accounting for similarity of $-90°$ and $+90$ orientations and taking the absolute value of all fiber measurements, our orientation data was not expected to follow a Gaussian distribution. Therefore, for the fiber alignment analysis, the Kruskal-Wallis nonparametric test was used and the Dunn's method for multiple comparisons was applied to find the statistical difference between the specimens. Histograms of the fiber alignment were using R (The R project, Vienna, Austria).

For the interdigitation index and mechanical properties comparison, correlations were calculated and tested for statistical significance by using linear regression model. Bonferroni corrections were used to obtain a corrected p value ($p\_corrected$) and adjust for the multiple comparisons.[2]

RESULTS

Neonatal to 18-Month-Old Fiber Alignment

Qualitative and quantitative measures show differences between ages for the coronal suture histology sections. In all neonate samples (Fig. 3a), the suture mesenchyme appears very disorderly with the fibers arranged in a net-like pattern. The only areas that show substantial alignment in the neonate samples are at the border regions between the mesenchyme and dura mater or pericranium. As the suture fibers

become more aligned in 9 and 11-month-old specimens, a transformation appears to occur from the innermost portion of the mesenchyme and develops outward. In the 9-month-old (Fig. 3b), the fibers at the center of the suture are more densely arranged and begin to align. The 11-month-old sample (Fig. 3c) exhibits the same increased alignment in the center of the suture and disorder at the bone front. Finally, in the 18-month-old sample (Fig. 3d), the suture contains locally aligned fibers throughout the entire mesenchyme, though the overall orientation varies relative to the bone. In the 18-month-old suture, there are distinct anchor points at which the collagen fibers connect the bone and suture mesenchyme. The suture is also much narrower due to the encroaching bone fronts and already there is an increase in interdigitation at this early age.

Measurement of the fiber alignment in the suture mesenchyme showed a general trend of increased local fiber alignment between the neonate specimen and the 18-month-old specimen (Table 1). A frequency distribution data plot from two example viewing frames (Fig. 4) demonstrates the difference in arrangement of fibers between the neonate and 18-month-old coronal sutures. The neonate suture has a much greater range of angle deviations, with a maximum angle deviation of 90° and a more even distribution of all possible fiber angles. In contrast, the 18-month-old sutures had the greatest angle deviation of only 47° and the histogram shows strong evidence of fiber alignment.

The combined average angle deviation measured in the 18-month-old, 16.2° ± 5.2°, was significantly lower than the neonate, 32.2° ± 6.9° ($p < 0.0001$), based on the Kruskal-Wallis test (Fig. 5). Although the 11-month-old and 9-month-old samples had a lower average angle deviation, 26.6° ± 3.7° and 25.2° ± 6.8° respectively, the change was not significant relative to the 18-month-old and neonate samples. Furthermore, though the neonate samples had a larger mean angle deviation than all other ages, the measurement of 32.2° would not be considered as a random fiber orientation of 45°. Additionally, when the data is separated into three age groups—neonate, mid-range (containing both the 9 and 11-month-old), and 18-month-old—the mean angle deviation is still only statistically significant when comparing the neonate and 18-month-old ($p < 0.0001$).

To verify the significance of these differences, we found no correlation ($R^2 < 0.001$) between the number of fibers measured, 95 ± 23 fibers, and the mean angle deviation when compared in a linear regression model, which eliminates possible bias caused by the number of fibers present or measured in any viewing frame. Finally, there were no significant differences between the mean angle deviations of the two neonate specimens

nor between any samples from the same specimen, demonstrating the age-specificity of the results observed.

6-Year-Old Suture Interdigitation

The sinuosity index varied from 1.14 to 3.18 with an average index of 1.86 ± 0.60 (Table 2). Further observation of the suture micro-CT slides showed a large amount of variation across one suture, possibly indicating the one sinuosity measurement could not accurately represent the three-dimensional suture morphology. The surface area interdigitation index varied from 2.31 to 4.04 with an average of 3.25 ± 0.55.

The only statistically significant correlation (p_corrected = 0.011) between morphology and mechanical properties was comparing sinuosity to ultimate strain (Fig. 6). The positive trend between the two values had an R^2 value of 0.62. Though a similar correlation was observed when comparing the surface area interdigitation and ultimate strain, $R^2 = 0.32$, the regression line was not significant. The surface area interdigitation index and sinuosity did not account for a significant portion of the variation and neither were correlated with any of the other mechanical data, including the elastic modulus and energy absorbed. The surface area interdigitation index was consistently larger than the sinuosity measurement for each suture and the correlation between the two was $R^2 = 0.28$ and was not significant.

DISCUSSION

This study examined the relationship between morphology and mechanical properties of the human suture and how the morphology changed with age. The motivation for this work arises from the belief that morphology might impact mechanical behavior of the sutures[11,19] and thereby impact the biomechanical behavior of the skull. Despite this longstanding belief, no study has examined both mechanical properties and morphology of the suture. As such, it has not been possible to develop models to predict these mechanical responses.

Neonatal to 18-Month-Old Fiber Alignment

The fiber alignment results show a significant increase in arranged fibers within the coronal suture from birth to 18 months and confirm our hypothesis that the morphology and fiber structure of the suture change dramatically with age within the first year and half of life. Currently no studies have quantified the
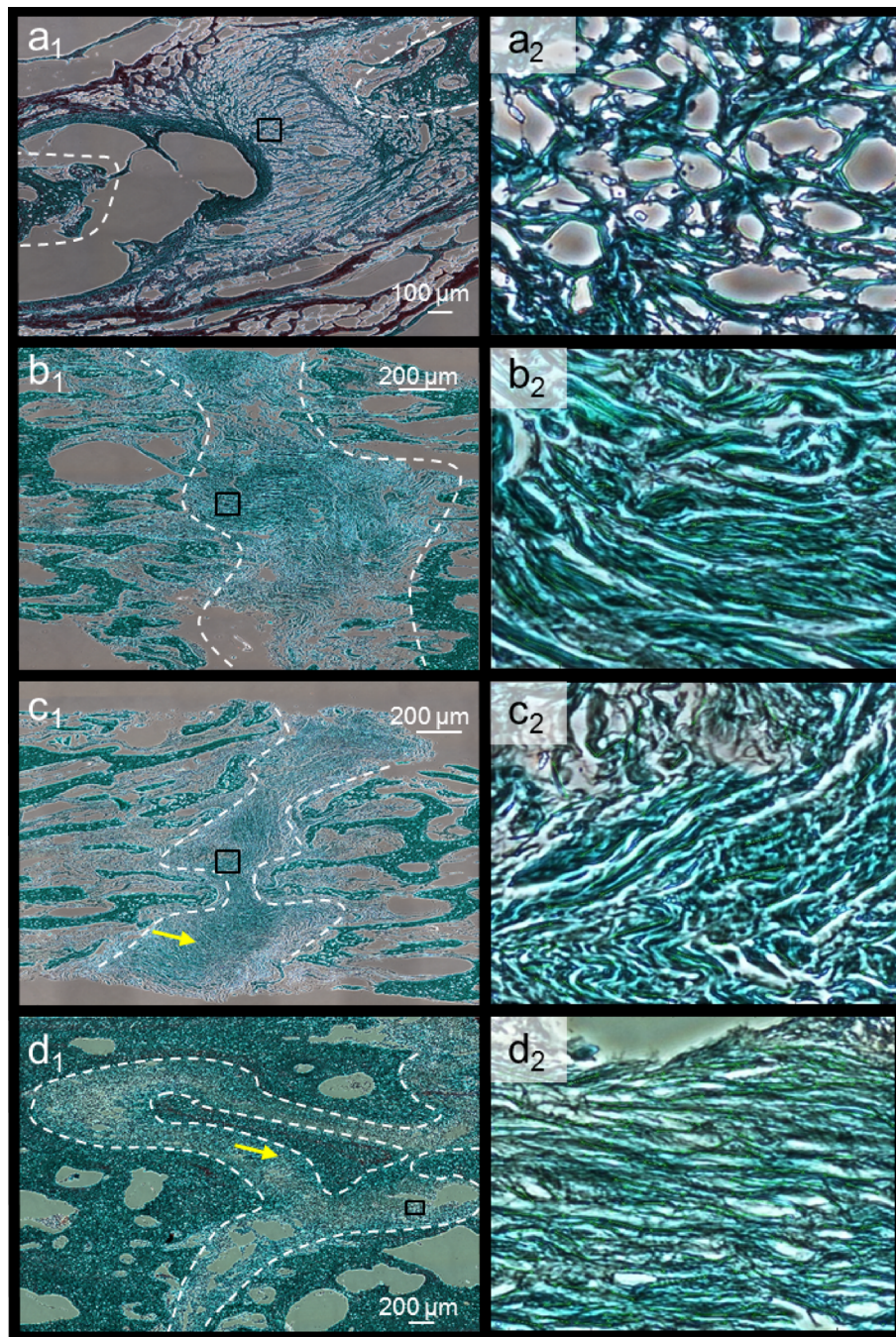
FIGURE 3. Suture samples (Masson's Trichrome under transmitted light microscopy) Bone edges are outlined with dashed white lines. (1) Reduced magnification to show bone fronts and suture mesenchyme. (2) Example 150 μm × 150 μm viewing frame per age. (a) Neonate, showing the net-like arrangement of fibers in the mesenchyme (b) 9-month-old, displaying an increase in arranged fibers though still lack of order at the bone interface (c) 11-month-old, similar to the 9-month-old, showing increase in arranged fibers specifically in the bottom portion of the suture shown by arrow (d) 18-month-old, suture space narrows and is more clearly defined by bone edge and fibers are more aligned shown by arrow.

alignment of fibers within the suture joint, though many have offered a qualitative assessment. Previous studies observed arranged fibers in porcine sutures, noting obliquely aligned fibers with reference to the bone face that were hypothesized to resist compressive strain.[22] In the pediatric specimens, we observed a si-milar pattern in fibers directly attached to the bone front, though only in the 18-month-old. Our work shows a significant change in the fibers within the su-ture in early development, supporting the observation from Coats and Margulies, which noted the impor-tance of obtaining age-specific material property data

TABLE 1. Fiber alignment results.

Specimen	Coronal suture sample	Viewing frame	N (fibers measured)	Mean angle deviation (per frame)	Mean angle deviation (per slide)
Neonate 1	Left	a	126	31.29	32.1° ± 3.7
		b	106	37.24	
		c	111	30.88	
		d	108	33.8	
		e	97	27.2	
	Right	a	81	27.09	32.6° ± 8.8
		b	100	29.25	
		c	60	46.43	
		d	102	24.6	
		e	78	35.68	
Neonate 2	Left	a	54	40.89	32.0° ± 12.5
		b	81	37.7	
		c	67	23.06	
		d	85	14.61	
		e	105	43.49	
	Left	a	109	25.48	30.7° ± 5.2
		b	106	36.92	
		c	78	25.11	
		d	129	32.63	
		e	127	33.45	
	Left	a	80	37.17	33.4° ± 3.1
		b	128	35.18	
		c	93	29.23	
		d	69	31.77	
		e	123	33.68	
9-month-old	Right	a	89	32.65	25.2° ± 6.8
		b	100	19.69	
		c	64	28.68	
		d	74	28.59	
		e	108	16.5	
11-month-old	Left	a	63	26.67	26.6° ± 3.6
		b	123	22.4	
		c	80	23.7	
		d	91	30.81	
		e	56	29.46	
18-month-old	Unknown	a	66	15.7	20.5° ± 3.7
		b	87	17.07	
		c	98	22.99	
		d	120	23.3	
		e	99	23.21	
	Unknown	a	129	12.13	11.9° ± 1.0
		b	151	11.73	
		c	125	10.79	
		d	113	11.36	
		e	93	13.37	

in pediatric specimen.[4,16] Even within the age gap of less than two years, the morphology of the suture changes significantly from a neonate to an 18-month-old.

The increase in arranged fibers observed in the suture could be due to the different roles of the suture during the development and growth of the pediatric skull. Our observations of the net-like pattern of the suture fibers in neonates would facilitate the necessary flexibility the skull needs to pass through the birth canal.[5] The increase in alignment with age may first serve as resistance to tensile strain, as seen in porcine sutures.[9] The tension within the suture joints has been presumed to instigate bone growth, a necessary function of the growing pediatric skull, and increase interdigitation, which we observed in the histology samples from the 18-month-old.[22] Ultimate ossification of cranial sutures, occurring between 22–26 years in humans, largely increases the strength of the skull (Cohen 2000). By increasing in strength and resistance
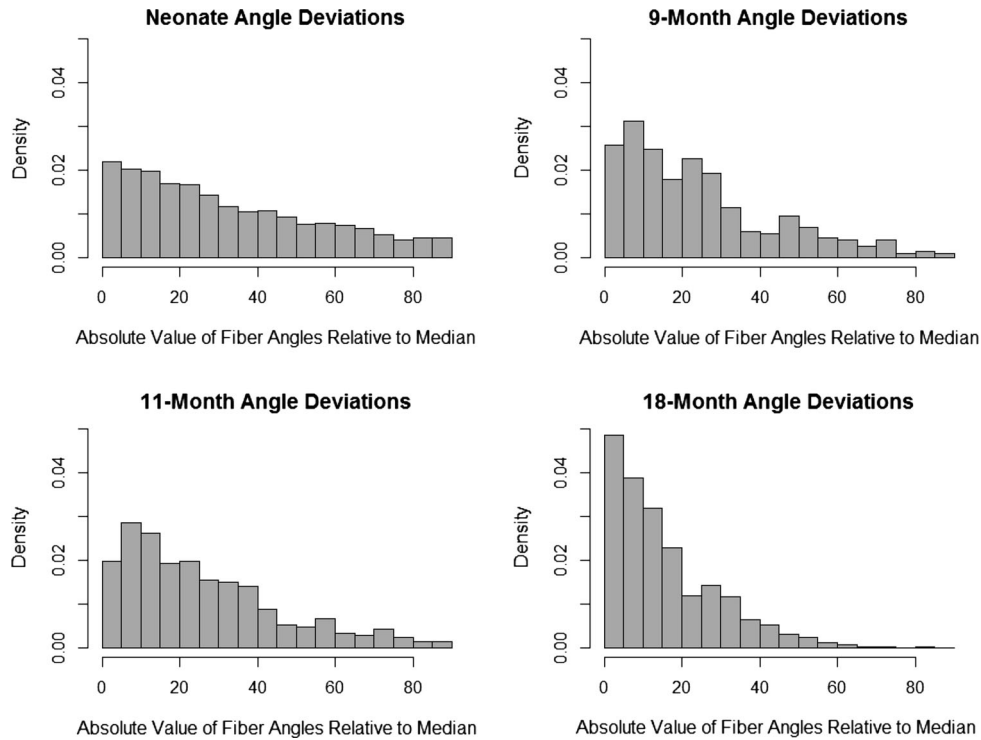
FIGURE 4. Histogram of fiber angle deviations relative to median slope by age category. Each histogram represents the angle deviation of each fiber from the median angle measurement across all samples and viewing frames for each age group. All plots have an area of 1 to allow comparison independent of the number of fibers measured or number of specimen used. The neonate samples have substantially larger variance than the 18-month-old samples, while the 9 and 11-month-old samples are more similar to one another and visually appear as a midpoint between the youngest and oldest age category.
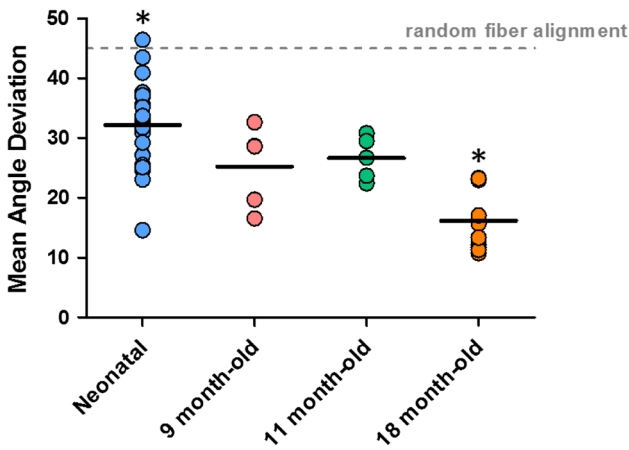

FIGURE 5. Average angle deviation decreases with age. Each point represents one viewing frame randomly selected from a suture sample, five samples per coronal suture section. Black bars indicate mean angle deviation from the median comparing all viewing frames within each age group. The mean deviation was $32.2° \pm 6.9°$ in the neonatal samples, $25.2° \pm 6.8°$ in the 9-month-old sample, $26.6° \pm 3.6°$ in the 11-month-old sample, and $16.2° \pm 5.2°$ in the 18-month-old sample. Grey dashed line indicates completely random orientation of $45°$. *is used to denote that the statistical difference between the neonates and the 18-month-old ($p < 0.05$).

to deformation, the skull with fused sutures can serve its role post-development by protecting the brain from injury.[4]

6-Year-Old Suture Interdigitation

Contrary to our hypothesis, a significant correlation ($p < 0.01$) was found between sinuosity and ultimate strain, but no other relationship between morphology and mechanical properties were identified (Fig. 6). This correlation suggests that a more interdigitated suture will deform more before ultimate failure than less interdigitated sutures. The ability to experience larger deformation can be explained by the variation of fiber direction associated with higher interdigitation. It is expected that under tensile stress from bending, the primary fibers to fail will be those experiencing tensile stress and aligned parallel to the direction of the experienced stress. Other fibers, though tightly aligned between the two bone faces, may be oriented perpendicular to the applied stresses due to the interdigitation and therefore would resist shear. As the initial fibers in tension fail, the load is transferred to the remaining

TABLE 2. Suture interdigitation results.

Coronal suture sample	Sample	Sinuosity	Surface area interdigitation index	Width (mm)	Height (mm)	Elastic MODULUS (GPa)	Ultimate strain (mm/mm)	Ultimate stress (MPa)	Yield strain (mm/mm)	Yield Stress (MPa)	Energy Absorbed (J)
Left	1	1.14	2.45	4.33	3.93	1.1126	0.0285	25.23	0.0285	25.23	17.91
Left	3	1.39	3.04	6.06	3.28	0.9255	0.0233	19.67	0.0233	19.67	17.4
Left	4	1.74	3.07	5.46	3.56	0.9794	0.0341	24.67	0.0282	23.71	44.2
Left	6	1.78	2.9	5.46	3.08	0.6082	0.0298	14.86	0.0281	14.56	25.14
Left	7	2.36	3.48	5.07	3.503	0.719	0.0453	30.21	0.0453	30.21	42.52
Right	1	1.47	2.71	4.62	4.12	1.0864	0.028	26.37	0.028	26.37	27.13
Right	2	1.57	2.45	3.38	3.38	0.6911	0.0319	18.64	0.0291	18.22	12.73
Right	3	1.17	4.00	3.84	3.02	2.0438	0.0284	47.71	0.0252	45.3	17.06
Right	4	2.34	3.88	3.34	3.08	1.095	0.0397	33.81	0.0332	31.7	24.65
Right	5	1.84	3.58	3.61	3.35	0.9393	0.0365	24.43	0.0273	22.46	19.36
Right	6	2.37	3.63	3.79	3.35	0.6595	0.0285	17.28	0.0285	17.28	13.9
Right	7	3.18	3.74	4.01	3.06	0.8881	0.0459	25.43	0.0275	21.2	30
Sinuosity (R^2)			0.28			0.19	0.62	0.02	0.15	0.05	0.13
SA inter index (R^2)		0.28				0.14	0.21	0.32	0.02	0.24	0.01

All samples were from one 6-year-old specimen. The correlations between sinuosity and suture area interdigitation index, and the mechanical properties are shown in the last two rows. Only the correlation between ultimate strain and sinuosity was found to be significant (p_corrected = 0.011). All the other correlations were not significant ($p > 0.05$).
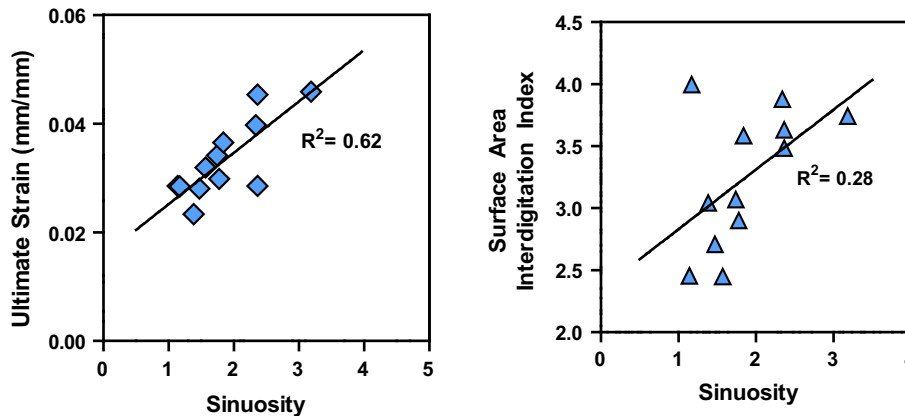

FIGURE 6. Ultimate strain is significantly correlated with sinuosity and can predict the ultimate strain of the suture through linear regression (p_corrected = 0.011) (left). The weak correlation between the sinuosity (right) (the 1-D measurement from the skull surface) and the surface area interdigitation (the 2-D measurement at the bone-suture interface) is not significant.

fibers, including those that normally serve to oppose shear. Lynch proposed such a theory observing that collagen fibers loaded in shear, or transverse to the applied force, are dependent on extrafibrillar matrix or cross-linking fibers to bear the applied load.[14] The varying orientation allows for the subsequent transfer of force to the remaining fibers, meaning the suture will not fail at once, and more interdigitated sutures could maintain a higher deformation before failing. This was also observed in Davis et al., as the suture samples tested did not completely rupture during failure in the four-point bend test, though all the diploic and cortical bone samples ruptured to failure.[6] This provides an advantage in that the bone could fail in its load bearing ability and still be connected to allow the fracture to easily heal without large displacements from the original location.

Results of the current study suggest that an increase in interdigitation, and potential varied fiber direction across the entire suture, could provide two competing effects to the suture. First, increased interdigitation increases the surface area available for the collagen fibers of the suture mesenchyme to anchor to the bone, contributing to an increase in suture strength measured as yield stress. Simultaneously, interdigitation alters some fibers' orientation from tension to shear, which increases the ultimate strain, but decreases suture strength measured as yield stress. Six-year-old pediatric sutures are 10–25% of the stiffness of the surrounding cranial bone and could be considered

vulnerable regions on the pediatric skull during development.[6] Nevertheless, the suture mesenchyme allows for remodeling during growth and development, but still contributes to the skull's resistance to overall failure.

Additionally, though the sinuosity and surface area index were correlated, the relationship was not significant, and therefore the index measurement from the skull surface does not indicate the level of interdigitation within the suture (Fig. 6). This observation is consistent with those made by Markey and Marshall who also noted that the sinuosity was not indicative of the amount of interdigitation observed from a cross-sectional view of the suture.[18]

Limitations in our histological analysis mainly derive from limitations with the tissue itself. Ideally, analysis would occur immediately post-mortem, which was not possible since extensive imaging and testing needed to be performed prior to histological analysis. Nevertheless, the collagen orientation, an extracellular product, and bone interdigtiations of the suture were preserved for the rigors of this study despite the time delay between when the samples were cut and analyzed. Second, due to the rarity of pediatric human cadavers, our histological study was limited to one specimen per age apart from the neonatal age and four specific ages from 9 to 18 months-old and the interdigitation calculations were performed on samples from only one 6-year-old specimen. Third, the younger specimens have not been mechanically tested. Since the suture of the younger specimen were unable to support a bending moment, a different testing method was need to mechanically test the sutures—this would consider beyond the scope of this study. Fourth, the mechanical properties reported for the 6-year-old are for the bulk mechanical properties the composite suture structure not the individual fibers. Fifth, the mechanical properties of the 6-year-old suture were calculated assuming that the suture behaved like a straight beam with a uniform cross section. However, the initial curvature of the samples were greater than five times the thickness of the samples and hence should have an insignificant effect.[10] Sixth, this study only focused on the properties of the coronal suture which was due to the small number of samples that were able to be obtained from the pediatric skull. Hence, this study only did histological sutures of the coronal sutures from the same specific area of the skull. Additionally, previous work by Davis *et al.* showed that the mechanical properties were not statistically different across suture locations.[6] The last limitation is that multiple measurements were taken for each specimen, hence the statistical variations shown in Fig. 5 may represent intra specimen variation rather than changes with age. The trends seen with age are predicated on the assumption that each specimen at each age is representative of their respective populations. Due to the paucity of pediatric tissue specimens, this is not an uncommon assumption in pediatric cadaver studies.[6] Regardless, this finding should be considered preliminary until this trend can be evaluated with more specimens at each age group.

CONCLUDING REMARKS

This study quantified the coronal suture geometry and assessed the effect of morphological variations on the mechanical properties of the suture. The results showed a statistically significant increase in locally arranged fibers of the suture mesenchyme in young pediatric specimens from newborns to 18 months old, with the average deviation decreasing from $32.2°$ to $16.2°$ ($p < 0.0001$). This progressive increase in fiber alignment may provide the initial steps leading to the stiffening and eventual fusion seen in adult sutures. Additionally, the results showed a statistically significant correlation between the sinuosity of the suture and the ultimate strain ($R^2 = 0.62$, p_corrected $= 0.011$), suggesting that an increase in interdigitation allows the suture a better ability to sustain deformation before complete rupture. However, there was no other correlation between the sinuosity index or the surface area interdigitation index and the other mechanical properties measured.

REFERENCES

[1]Beresford, W. A. Cranial skeletal tissues: diversity and evolutionary trends. In: The Skull, edited by J. Hanken and B. K. Hall, 2:69–130. Patterns of Structural and Systematic Diversity: University of Chicago Press, 1993, pp. 69–130.

[2]Bland, J. M., and D. G. Altman. Multiple significance tests: the Bonferroni method. *BMJ* 310:170, 1995.

[3]Bradley, J. P., J. P. Levine, C. Blewett, T. Krummel, J. G. McCarthy, and M. T. Longaker. Studies in cranial suture biology. In vitro cranial suture fusion. *Cleft Palate-Craniofacial J.* 33:150–156, 1996.

[4]Coats, B., and S. S. Margulies. Material properties of human infant skull and suture at high rates. *J. Neurotrauma* 23:1222–1232, 2006.

[5]Cohen, M. M. Sutural biology. In Craniosynostosis: Diagnosis, Evalutation, and Management, edited by J. M. Michael Cohen and R. E. MacLean. New York: Oxford University Press, 2000, pp. 11–22.

[6]Davis, M. T., A. M. Loyd, Shen H-yH, M. H. Mulroy, R. Nightingale, *et al*. The mechanical and morphological properties of 6-year-old cranial bone. *J. Biomech.* 45:2493–2498, 2012.

[7]Gelse, K., E. Pöschl, and T. Aigner. Collagens—structure, function, and biosynthesis. *Adv. Drug Deliv. Rev.* 55:1531–1546, 2003.

[8]Herring, S. W. Sutures—a tool in functional cranial analysis. *Cells Tissues Organs* 83:222–247, 1972.

[9]Herring, S. W. Sutures and craniosynostosis: a comparative, functional, and evolutionary perspective. In: Craniosynostosis: Diagnosis, Evaluation, and Management, edited by J. M. Michael Cohen and R. E. MacLean. New York: Oxford University Press, 2000, pp. 3–10.

[10]Hibbeler, R. C. *Mechanics of Materials*. Upper Saddle River: Prentice Hall, 2003.

[11]Jaslow, C. R. Mechanical properties of cranial sutures. *J. Biomech.* 23:313–321, 1990.

[12]Jaslow, C. R., and A. Biewener. Strain Patterns in the horncores, cranial bones and sutures of goats (Capra hircus) during impact loading. *J. Zool.* 235:193–210, 1995.

[13]Johansen, V. A., and S. H. Hall. Morphogenesis of the mouse coronal suture. *Cells Tissues Organs* 114:58–67, 1982.

[14]Lynch, H. A., W. Johannessen, J. P. Wu, A. Jawa, and D. M. Elliott. Effect of fiber orientation and strain rate on the nonlinear uniaxial tensile material properties of tendon. *Trans. ASME* 125:726–731, 2003.

[15]Maikos, J. T., R. A. I. Elias, and D. I. Shreiber. Mechanical properties of dura mater from the rat brain and spinal cord. *J. Neurotrauma* 25:38–51, 2008.

[16]Margulies, S. S., and K. L. Thibault. Infant skull and suture properties: measurements and implications for mechanisms of pediatric brain injury. *J. Biomech. Eng.* 122:364–371, 2000.

[17]Markey, M. J., R. P. Main, and C. R. Marshall. In vivo cranial sutures function and suture morphology in the extant fish Polypterus: implications for inferring skull function in living and fossil fish. *J. Exp. Biol.* 209:2085–2101, 2006.

[18]Markey, M. J., and C. R. Marshall. Linking form and function of the fibrous joints in the skull: a new quantification scheme for cranial sutures using the extant fish Polypterus endlicherii. *J. Morphol.* 268:89–102, 2007.

[19]Markey, M. J., and C. R. Marshall. Terrestrial-style feeding in a very early aquatic tetrapod is supported by evidence from experimental analysis of suture morphology. *Proc. Natl Acad. Sci. U.S.A.* 104:7134–7138, 2007.

[20]Persson, M., B. C. Magnusson, and B. Thilander. Sutural closure in rabbit and man: a morphological and histochemical study. *J. Anat.* 125:313–321, 1978.

[21]Pritchard, J. J. The structure and development of cranial and facial sutures. *J. Anat.* 90:73–86, 1956.

[22]Rafferty, K. L., and S. W. Herring. Craniofacial sutures: morphology, growth, and in vivo masticatory strains. *J. Morphol.* 242:167–179, 1999.

[23]Rossert, J., and B. Crombrugghe. Type I collage: structure, synthesis, and regulation. In: Principles of Bone Biology, edited by J. P. Bilezikian, L. G. Raisz, and G. A. Rodan, 2002, pp. 189–210.

[24]Slater, B. J., K. A. Lenton, M. D. Kwan, D. M. Gupta, D. C. Wan, and M. T. Longaker. Cranial sutures: a brief review. *Plast. Reconstr. Surg.* 121:170e–178e, 2008. doi: 10.1097/01.prs.0000304441.99483.97.

[25]Xu, Y., P. Malladi, M. Chiou, and M. T. Longaker. Isolation and characterization of posterofrontal/sagittal suture mesenchymal cells in vitro. *Plast. Reconstr. Surg.* 119:819–829, 2007.